2014 International Conference on Unmanned Aircraft Systems (ICUAS)
May 27-30, 2014. Orlando, FL, USA

Design and Development of a Semi-autonomous Fixed-Wing Aircraft with Real-time Video Feed

Cody Torno†, Christoph Hintz, and Luis Rodolfo García Carrillo

Abstract— **In recent years, the understanding and development of Unmanned Aircraft Systems (UAS) has grown exponentially. With technological advancements in the fields of integrated circuits and battery polymers it is now possible to produce UAS that can provide benefits far outside their initial military purposes. Despite this, there are still very few developed UAS that can exploit such technological advancements. Several large scale vehicles (>4 m) utilize gas propeller-driven systems, which enables long endurance flights and applications of reconnaissance, surveying, and high altitude sensor testing. Unfortunately, these are exponentially expensive to purchase, maintain, and operate. On the other hand, there are mini-UAS (m-UAS)in production; most of them are focused on copter designs for study of stabilization and path planning software. m-UAS are a viable option for low endurance, altitude, and payload objectives due to battery limitations and constant adjustment of thrust for directional stabilization and maneuvering. The research presented here focus on the design and development of a fixed-wing aircraft that serves as a viable option between UAS and m-UAS platforms, with the purpose of merging the strengths of both systems into a low-cost, high versatility vehicle. The proposed UAS considers low-level autopilot capabilities for stabilized flight, with a minimum flight time of 60 min and 60 Km distance. Additionally, a 3-axis gimbal stabilized camera system is designed and implemented to produce steady video stream to a ground control station.**

Index Terms— **Unmanned Aircraft Systems, Dynamic Model, Low-level autopilot**

I. INTRODUCTION

In recent years, Unmanned Aircraft Systems (UAS) or Remotely Piloted Vehicles (RPVs) have developed far past their initial applications in military settings. This is due to the large influx of new technological advancements, making these vehicles less expensive and more reliable than their manned predecessors [1] A UAS has several characteristics that provide benefits over traditional manned aircraft. With the manned flight systems removed from the cockpit and replaced with light weight on-board computer systems, the vehicle does not experience any major design constraints. UAS can take the form of fixed-wing, rotary-wing, or lighter-than-air vehicles that can range in sizes from 0.1 m to 15 m [2]. A fixed-wing UAS platform has a large advantage over similar manned aircraft, e.g., their ability to offer long flight durations and superior flight altitudes with less acoustic propulsion systems, avoiding visual and radar detection [2] [1]. UAS have many applications that include governmental uses in intelligence gathering, surveillance, and Reconnaissance (ISR) and homeland security [3]. The civil sector is greatly interested in the platforms with potential to be utilized for geo-location or surveying, assessment of natural disasters, research and testing platforms academia, as well as several applications in lad management, commercial, and earth science studies [4]. The main disadvantages of these platforms are the logistical footprint made due to the requirement of Launch and Recovery Systems (LRS). LRS requires a large ground crew to facilitate proper operations and can involve costly launch mechanisms to facilitate initial flight speed, such as runways or pneumatic catapults [2].

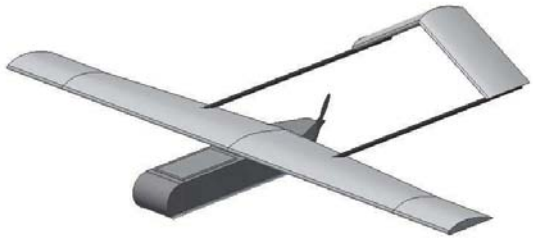

Fig. 1. Fixed-Wing UAS

TABLE I
UAS CATEGORIES DEFINED BY THE DEPARTMENT OF DEFENSE.

UAS Category	Max Gross Takeoff Weight	Normal Operating Altitude (ft)	Airspeed
Group 1	< 20 pounds	<1200 AGL	<100 knots
Group 2	21 - 55 pounds	<3500 AGL	<250 knots
Group 3	< 1320 pounds	<18,000 MSL	
Group 4	> 1320 pounds		Any Airspeed
Group 5		>18,000 MSL	

The U.S Department of Defense (DoD) currently categorizes RPAs into five groups, which can be seen in Table I. It has been identified by the department of commerce that Group 1 will dominate civil-use UAS markets due to their low operating altitude, commercialization potential, and low logistical footprint. However, as of 2010, majority of commercialized vehicles fall outside of this category [5]. As the FAA moves towards UAS tolerant policies, the integration and development of this UAS category in NAS will greatly expand civil interest.

There are several limitations of conventional platforms that

†The work of the first author is supported in part by the McNair Scholars Program, Texas A&M University - Corpus Christ

C. Torno, C. Hintz, and L.R. García Carrillo are with the Unmanned Systems Laboratory, School of Engineering and Computing Sciences, Texas A&M University - Corpus Christi, Corpus Christi, TX 78412 USA. e-mail: {ctorno,chintz}@islander.tamucc.edu, L.R. García Carrillo e-mail: luis.garcia@tamucc.edu

provide reason for development of alternative solutions. Most fixed-wing UAS in operation have large wingspans and use gas power plants for propeller-driven propulsion. Although these systems allow for long endurance flights and large application basis, they usually flight at altitudes and speeds that limit their applications in the civil sector. In addition, these platforms are also exponentially expensive to purchase, maintain and operate, limiting the payback potential of the system in civil use [5]. The most important limitation is the required logistics that goes into these larger UAS flights.

In order to provide an alternative platform for the growing interest of the civil sector and higher education institutions, the present research presents the development of a fixed-wing platform adhering to the current and future FAA restrictions on UAS handling and operations. There are several objectives for this platform, which range from aerodynamic capabilities to payload characteristics. The proposed UAS will provide real-time video feed for use in the assessment of platform potential and design flaws. The platform will have the capability of maintain level flight with payloads as large as 3 kg, while operating using an all-electric propulsion system. The electrical power plant system is designed to optimize the battery life of the UAS, increasing endurance to over 60 min. The payload system is composed of a three axis gimbal stabilized GoPro 3 Hero® camera, allowing for a high definition video transmission.

The organization of this manuscript is as follows. Section II presents the available commercially and research based platforms similar to that proposed in this manuscript. Section III discusses the RPV platform design in detail, including aerodynamic simulation of wing components. Section IV provides a detailed dynamic model of the RPV platform in regards to pitch, roll and yaw dynamic movements. Section V develops the understanding of gimbal assisted real-time video and potential of system. Section VI demonstrates the experimental platform and the details of the components required for experimental flight. Section **??** provides results of simulations and real time experimental flight data. Finally some conclusions are presented in Section VII

II. RELATED WORK

A. Commercially Available Platforms

Several commercially available platforms are available for purchase with autonomous flight capabilities. AeroVironment [13] has several group 1 classification UAS platforms that were initially developed for the military. However, they have recently been awarded a *restricted category* rating from the FAA to allow for commercial purposes. The RQ-20A Puma AE (all environment) closely resembles the platform proposed in [13]. It has a wingspan of 2.8 m with an overall weight of 6 kg and endurance of 3.5 hours. The payload is gimballed, housing an electro-optic and inferred camera system. The fuselage is completely waterproof, quickly hand launched, and with autonomous landing capabilities. Another AeroVironment UAS platform of smaller size is the RQ-11B Raven [13]. It is the most widely used UAS in the world. The platform has the same gimballed payload as the Puma, however its wingspan of 1.4 m and 60 min flight time are significantly less. The costs of these systems are upwards of $250,000 and are far out of the reach of most civil and research institutions.

Another commercial UAS system that has similar flight characteristics of the proposed platform is the Marcus Zephyr 2 [14]. It is a flying wing configuration with a wing span of 1.4 m and endurance of 60 min. The cost of this vehicle is significantly cheaper than the military grade AeroVironment platforms at $13,000. However this platform provides limited payload alternations, and requires extensive post processing to calculate the point and location of imagery due to stationary payload systems [14].

B. Research Developed Platforms

With the development of low-level autopilot systems, it has been possible for low cost research based platforms to be developed to study various aspects of flight and system control. Many of the platforms being used are retrofitted R/C planes or in-house designed flying wing designs [6]. Both of these provide minimal payload bays and reduce the versatility of the vehicle to system control and stability algorithm testing [7] [21] [6].

III. DESIGN OF RPV PLATFORM

A. Design of the General Structure

The primary mission of the proposed fixed-wing system is to provide a semi-autonomous platform with real time video capabilities for various payload applications. The vehicle will continue to possess the attribute of use for development and study of low-level autopilot systems in low Reynolds number flights environments for future studies. The first step in the platform design was to establish the design constraints based on the mission criteria. Since this platform is proposed as a versatile payload platform, it is critical that the aircraft produce enough lift to support all systems including a range of optional payload systems for future studies. The fuselage must be hollow in design and accommodate all flight hardware, video system, and numerous payloads configurations. The platform must have the ability to cruise at altitudes of $>$100 m at speeds between 15 m/s 20 m/s for optimum video feed stabilization and transmission [4].

The wing-span of the vehicle must not exceed 2.5 m to allow for ease of transportation. The fuselage and wings connection must be dynamic to accommodate changes in center of gravity (CG) due to user payload preference. After initial designs it was determined that the fixed-wing RPV would have two sections: (i) the main wing/fuselage, and (ii) an anhedral V-tail connected by twin booms. This design can be seen in Figure 2. The RPV will be made entirely out of expanded polypropylene (EPP) with a 22 gauge aluminum inlay for structural support of the fuselage and components.

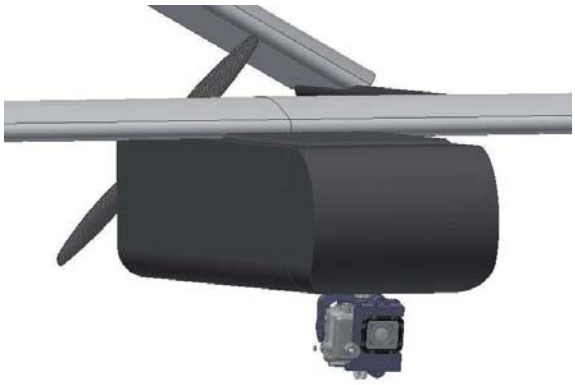

Fig. 2. The fuselage/payload platform design. A three axis gimbal stabilized GoPro 3 Hero® camera, allowing for a high definition video transmission is shown.

B. Design of the Wings and Flaperions

In order to be capable of flight and provide the flight characteristics of interest, several design issues had to be overcome. The first was the wing span for the main wing, which must be capable of providing enough lift for flight with the desired payload size, while remaining rigid enough to maintain lift characteristics when external forces such as gusting winds are applied. This wing was determined to resemble those of gliders planes, which have high wing area to payload weight [7]. In gliders, this ratio is critical due to them lacking propulsion and the need to maintain high lift to increase flight times. However, this ratio can be utilized to minimize the power consumption by the motor by needing majority of the motor's power to achieve altitude rather than maintain flight. The flight characteristics and lift of a wing is dependent on the airfoil design used. For this airframe's application, it is important that the airfoil design has a very high lift to drag ratio with a small percentage thickness to chord length ratio, aiming at reducing pressures during climbs [7]. The total lift requirement for the wing is dependent on the *all up weight* of the aircraft. The base weight avionics, payload, and airframe weight specifications can be seen in Table II.

During the development of an aerial vehicle, the aerodynamic properties of the vehicle are important aspects of the design. Since the *all up weight* of the design has been identified, it is possible to obtain the lift coefficient. It was calculated that at cruising speed, the lift coefficient for an all up weight of 2.212 kg would be 0.289. This low lift coefficient shows that there is significant lift to maintain this platform. The lift coefficient also plays a large role in the power requirements of the airframe during flight when related to drag coefficient. As this ratio increases, the flight and efficiency capabilities of the airframe are linearly increased. Since the vehicle will be flying at a height of around 100 m, we can assume atmospheric density values at sea level with low Reynolds numbers.

TABLE II

PLATFORM COMPONENTS WEIGHT

Avionics & Payload		Aircraft	
Component	Weight (kg)	Component	Weight (kg)
Ardupilot	0.023	EPP Foam	0.300
Gimbal System	0.250	Fuselage Alloy	0.150
GoPro® Hero 3	0.090	Spars	0.170
RC Receiver	0.040	Brushless Motor	0.180
Speed Control	0.033	Propeller	0.050
Video Transmitter	0.040	Glue/Hardware	0.050
Servo X 5	0.036		
Batteries	0.800		
Total	1.312	Total	0.900
		Total	2.212

TABLE III

XFLR-5 ANALYSIS RESULTS

Design	1	2	3	4
Airfoil	USNPS	USNPS	E214	E214
Dihedral	0°	5°	0°	5°
Wing Span (mm)	2500	2500	2500	2500
Wing Area (cm^2)	5530	5530	5530	0.150
CG (mm)	230	230	230	230
Velocity (m/s)	11.2	11.3	11.5	11.6
C_L	0.5115	0.4971	0.4820	0.4698
C_L/C_D	82.86	65.50	74.68	68.28
Stall Angle (α)	14.6	14.6	12.6	12.6

An important aerodynamic term to understand during development of results and deliverables is the angle of attack (a) [8], referring to the pitch angle that the airframe is experiencing with respect to the earth frame. The angle of attack is zero during stable flight at desired altitude, and refers to the vehicle not pitching up or down to change flight height. During launch/landing stages, the angle of attack is increased or decreased to reach desired altitude [9].

Using a wind tunnel flight simulation software called XFLR-5 [10], it is possible to simulate initial aerodynamic properties of airframes. The software makes it possible to conduct preliminary evaluations on several airfoil and platform designs to gain perspective on possible flight characteristics. XFLR-5 software runs foil and platform analysis based on lifting line theory and vortex lattice method [10], [4]. The resulting airfoil aerodynamic data for four conceptual platform designs were evaluated and the aerodynamic properties obtained can be seen in Table III.

Due to the manufacturing and equipment limitations, the airfoils of interest were the USNPS-4 and E214 []. These airfoils had relatively flat bottoms and allow for increased accuracy in replication to increase platform symmetry. In all designs considered, the wingspan was at the max constraint of 2.5 m which allowed analysis of airfoil and wing dihedral effects on aircraft performance. It was seen that as the dihedral angle of the main wing was increased in design

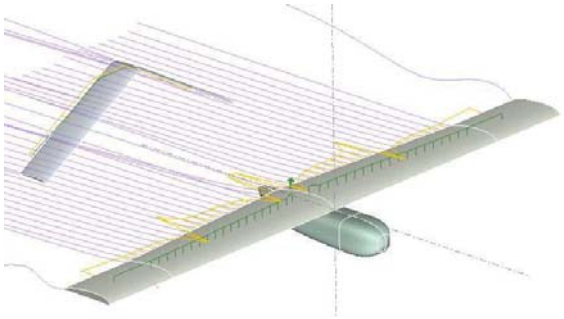

Fig. 3. XFLR-5 Analysis of Platform Iso View.

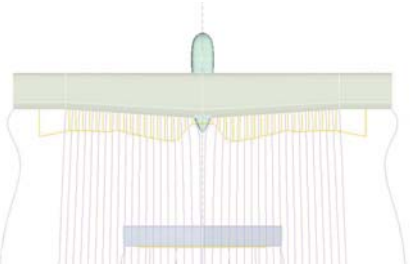

Fig. 4. XFLR-5 Analysis of Platform Top View.

2 and design 4, the lift properties and cruising speeds were reduced to some degree. This can be expected due to dihedral angles reduce the lift producing wing span area, however it provides an advantage of roll stability. After consideration of the designs, the USNPS-4 airfoil was chosen for the platform due to its low drag at cruising altitude, which greatly increased its lift/drag ratio.

The analysis using XFLR-5 can be seen in Figure 3. This program allowed for initial development of platform, however for accuracy, data will also be gathered using wind tunnel analysis. The addition of flaperons to the main wing were determined valuable based on the desire to decrease the velocity at two important sections of the flight path, at cruising altitude and during landing. This would allow for slower flight over target and minimize damage done during landing. XFLR-5 analysis of a 15° deflection in flaperons produced 50% increase in lift coefficient C_L and a 30% decrease in velocity 5.

IV. DYNAMIC MODEL OF RPV PLATFORM

The equations of motion for conventional fixed-wing aircraft can be derived by accounting for rigid-body kinematics, propulsion, gravitational, and aerodynamic forces. These non-linear and coupled equations can be linearized using first order Taylor series expansion to identify the aircraft dynamics. The equations of motion are taken in the body axis reference frame of the aircraft and assumes a flat Earth coordinate system. The rigid body dynamics consists of the inertial positions $[X, Y, Z]$, body-axis velocities $[u, v, w]$, attitude angles $[\phi, \theta, \psi]$ and body-axis angular rates $[p, q, r]$. The platform description presented in this manuscript represents a simplified model of the actual vehicle.

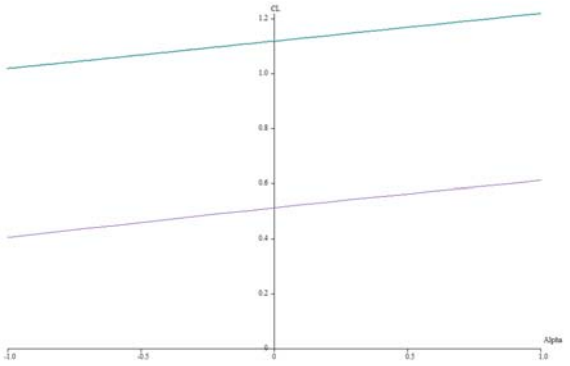

Fig. 5. Flaperons positioning with respect to lift coefficient.

The dynamic equations are linearized with the assumption of steady equilibrium flight conditions with throttle remaining constant. These 6 Degrees of Freedom (DOF) rigid-body forces and moments in the body frame are defined as τ_{RB} and is split into its force equations f_o^b and m_o^b

$$\tau_{RB} = \begin{bmatrix} f_o^b \\ m_o^b \end{bmatrix} = \begin{bmatrix} X \\ Y \\ Z \\ L \\ M \\ N \end{bmatrix} = \begin{bmatrix} \text{forward force} \\ \text{sideway force} \\ \text{vertical force} \\ \text{roll moment} \\ \text{pitch moment} \\ \text{yaw moment} \end{bmatrix} \tag{1}$$

These forces and moments are the sum of aerodynamic, gravitational, and actuated forces and moments (1). The system of equations can be broken down into component form

$$\begin{bmatrix} X \\ Y \\ Z \\ L \\ M \\ N \end{bmatrix} = \begin{bmatrix} m(\dot{U} - VR + WQ) \\ m(\dot{V} - UR + WP) \\ m(\dot{W} - UQ + VP) \\ I_{xx}\dot{P} - I_{xz}\dot{R} - I_{xz}PQ + (I_{zz} - I_{yy})RQ \\ I_{yy}\dot{Q} + (I_{xx} - I_{zz})PR + I_{xz}(P^2 - R^2) \\ I_{zz}\dot{R} - I_{xz}\dot{P} - I_{xz}QR + (I_{yy} - I_{xx})PQ \end{bmatrix} \tag{2}$$

The components in (2) form a set of six nonlinear differential equations with six unknown variables (U, V, W, P, Q, R) [11]. Each of these variables are represented dependently with these nonlinear equations of motion. The total solution for the system of equations can be obtained only by applying numerical integration to all equations for each given time step. The forces that act on the platform can be expanded to represent the aerodynamic forces due to(F_A), thrust (F_T), and gravity (mg) . The moments acting on the aircraft are generated from aerodynamic and thrust forces with respect to the aircraft CG. These expanded terms are

$$\begin{bmatrix} X \\ Y \\ Z \\ L \\ M \\ N \end{bmatrix} = \begin{bmatrix} mg\sin\Theta + F_{A_x} + F_{T_x} \\ -mg\cos\Theta\sin\Phi + F_{A_y} + F_{T_y} \\ -mg\cos\Theta\cos\Phi + F_{A_z} + F_{T_z} \\ L_A + L_T \\ M_A + M_T \\ N_A + N_T \end{bmatrix} \tag{3}$$

A. Aerodynamics

Aerodynamic forces are one of the major forces applied to an aircraft. They create moments that affect flight dynamics

heavily. Aerodynamic forces are composed of lift, drag, and side force, which generate moments with respect to the CG about X, Y, and Z axis. The aerodynamic forces can be related by their dimensionless coefficients. These coefficients can be found theoretically, or experimentally via wind tunnel testing. Specifically, they are found by multiplying the coefficients with the reference area S (m^2) and the dynamic pressure q (N/m^2) from Bernoulli's theorem for streamlined flow

$$q = \frac{1}{2}\rho V_T^2 \tag{4}$$

where ρ is the air density. The aerodynamic forces can then be written as

$$\begin{bmatrix} -X \\ Y \\ -Z \\ L \\ M \\ N \end{bmatrix}_{WIND} = \begin{bmatrix} qSC_D \\ qSC_Y \\ qSC_L \\ qSbC_l \\ qS\bar{c}C_M \\ qSbC_N \end{bmatrix} \tag{5}$$

These coefficients are heavily impacted by the aircraft shape, airflow angles, angular rates, and control settings. The platform presented here has a 30° anhedral V-tail without rudder controls. The control derivatiyes are therefore identified as ailerons (C_{δ_a}), flaps(C_{δ_f}), elevator(C_{δ_e}) and thrust(C_{δ_T}). The building up of the aerodynamic forces and moments as a sum of contributing components provides a convenient way of representation for a specified flight condition. They are associated with the stability and control derivatives in terms of independent parameters. The total definition of aerodynamic coefficients, including static and dynamic effects results in .

$$\begin{bmatrix} -X \\ Y \\ -Z \\ L \\ M \\ N \end{bmatrix} = q \begin{bmatrix} C_{L_o} + C_{L_\alpha}\alpha + C_{L_{\hat{q}}}\frac{q\bar{c}}{2V_T} + C_{L_{\dot{\hat{\alpha}}}}\frac{\dot{\alpha}\bar{c}}{2V_T}\dot{\alpha} + C_{L_{\delta_e}}\delta_e \\ C_{D_o} + \frac{(C_L - C_{L_o})^2}{\Pi e A R} + C_{D_\delta}\delta \\ C_{Y_\beta}\beta + C_{Y_{\hat{p}}}\frac{pb}{2V_T} \\ b(C_{l_\beta}\beta + C_{l_{\hat{p}}}\frac{pb}{2V_T} + C_{l_{\hat{r}}}\frac{rb}{2V_T} + C_{l_{\delta_a}}\delta_a) \\ \bar{c}(C_{M_o} + C_{M_\alpha} + C_{M_{\dot{\hat{\alpha}}}}\frac{\dot{\alpha}\bar{c}}{2V_T} + C_{M_{\hat{q}}}\frac{q\bar{c}}{2V_T} + C_{M_{\delta_e}}\delta_e) \\ b(C_{N_\beta}\beta + C_{N_{\hat{p}}}\frac{pb}{2V_T} + C_{N_{\hat{r}}}\frac{rb}{2V_T} + C_{N_{\delta_a}}\delta_a) \end{bmatrix} \tag{6}$$

These stability and control derivatives determine the aerodynamic characteristics of the platform presented. They can be estimated or identified through wind tunnel testing and flight data.

The kinematic equations are represented as shown in equation (7), with control of yaw motion not considered due to the geometry of tail. The stabilization of roll, pitch, roll rate, and pitch rate will ensure stability in yaw.

$$\begin{bmatrix} \dot{\phi} \\ \dot{\theta} \end{bmatrix} = \begin{bmatrix} p + \tan\theta(q\sin\phi + r\cos\phi) \\ q\cos\phi - r\sin\phi \end{bmatrix} \tag{7}$$

The coefficients in attitude update equations are

$$c_1 = \frac{(I_{yy} - I_{zz})Izz - I_{xz}^2}{I_{xx}I_{zz} - I_{xz}^2} \tag{8}$$

$$c_2 = \frac{(I_{xx} - I_{yy} + I_{zz})Ixz}{I_{xx}I_{zz} - I_{xz}^2} \tag{9}$$

$$c_3 = \frac{I_{zz}}{I_{xx}I_{zz} - I_{xz}^2} \tag{10}$$

$$c_4 = \frac{I_{xz}}{I_{xx}I_{zz} - I_{xz}^2} \tag{11}$$

$$c_5 = \frac{I_{zz} - I_{xx}}{I_{yy}} \tag{12}$$

$$c_6 = \frac{I_{xz}}{I_{yy}} \tag{13}$$

$$c_7 = \frac{1}{I_{yy}} \tag{14}$$

$$c_8 = \frac{(I_{xx} - I_{yy})Ixx - I_{xz}^2}{I_{xx}I_{zz} - I_{xz}^2} \tag{15}$$

$$c_9 = \frac{I_{xx}}{I_{xx}I_{zz} - I_{xz}^2} \tag{16}$$

The aircraft being modeled can then be represented in Appendix (1) in the wind-axes after small angle approximations. The coefficient for free stream airspeed is V_T, the angle of attack is α, the sideslip angle is β, D represents the drag force, L the lift force, Y the side force, F_T the thrust force produced by the engine, and Z_{TP} the offset from the CG in the body-frame z-direction. It is assumed that the airspeed V_T remains constant as it varies much slower than other system states.

V. REAL-TIME VIDEO SYSTEM

The video system was designed to serve as a benchmark test of gimbal operations and control. The main expectation for the system is to have 360° degree viewing angle and autonomous stabilization to compensate for change in vehicle orientation based on all three axes. Since the RPV is designated for several applications, it is expected that the camera system allow for different camera types. The camera system must be rugged and capable of withstanding damage during testing. As shown in Figure 6, the camera gimbal apparatus has been designed to be easily 3D printed to exact specifications and can easily be replaced.

The material is made of high density plastic and has three 2208 KV80 brushless gimbal motors to power orientation stabilization. The stabilization software is stored on a Quanum AlexMos brushless gimbal controller that receives input from the Ardupilot® and user input. This allows the ground control station to manually operate and maneuver the video system during stabilization to focus on different geographical locations. This system was chosen for its potential to be utilized for geo-lock and tracking applications, with the integration and coordination of the Autopilot and video system to alter flight path to allow continuous monitoring of points of interest.

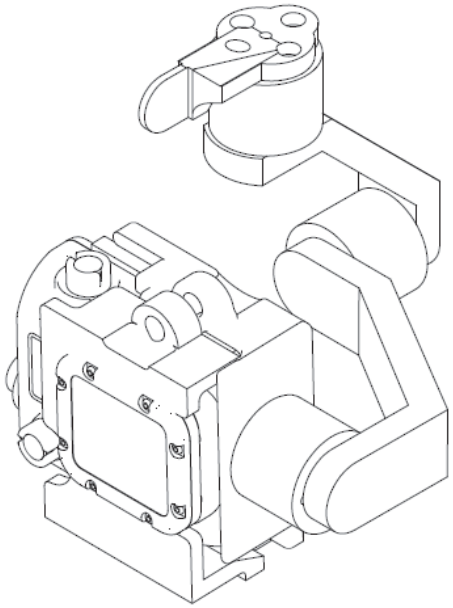

Fig. 6. 3D printed camera gimbal apparatus.

Fig. 7. Completed Airframe.

VI. The Experimental Platform

At this time, the experimental platform and its components are still being manufactured and assembled. The sections below show the progress of the experimental platform build at time of manuscript.

A. Airframe

The experimental platform has a wing span of 3.0 meters but could be reduced to 2.5 meters to reduce wing flexure. The fuselage is 0.5 m in length with front cone and motor connector, and will have a complete length of 0.65 m. It can be seen from (7) that the fuselage is made of basswood and depron foam. The toal vehicle weight is 4 kg which includes all components.

Fig. 8. Ground Station Computer.

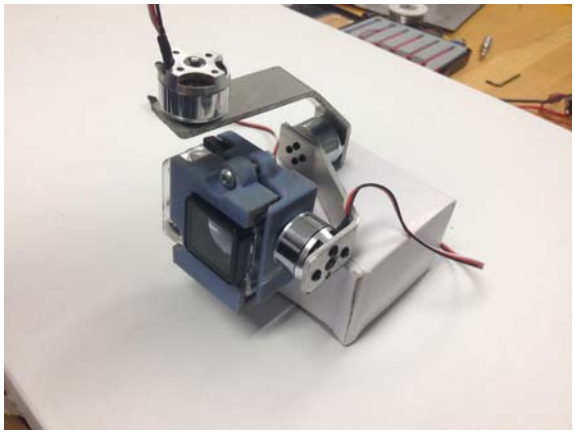

Fig. 9. 3D printed camera gimbal apparatus.

B. Ground Station

The ground station for the platform was developed using two dell 1907FPVt monitors and dell desktop computer that were dissembled to fit inside a weather-proof housing with dimensions of $0.914 \times 0.33 \times 0.152$ m (8). This allows the ground components to be completely portable and resistant to the elements. One of the screens will be devoted to the ground station software while the other is reserved for payload and telemetry data. The communication system from the ground station to the airframe will be an omni antenna that will allow for video reception for up to 5 km.

C. Payload

The payload system can be seen in figure (9). During the development it was determined that it was critical to keep the camera protected within its case. This added weight and increased the weight of the payload to 0.275 kg due to this adaptation, however its durability was greatly increased.

VII. CONCLUSIONS

The design of a high versatile, low cost fixed-wing UAS for the use in the academic and future civil applications provides several design and cost challenges. It is important

that the reliability of the vehicle is not compromised due to the materials and software used. Future work will be devoted to the simulation and testing of the UAS and low level autopilot software. The control system structure and design will be developed in order to accurately respond to the aircrafts on board attitude sensors. After the completion of the airframe and ground station, experimental testing will be conducted along with wind tunnel testing to provide comparison to simulations.

REFERENCES

[1] R. Austin, *Unmanned Aircraft Systems: UAVs design, development and Deployment*, Chapter 26-27, pp.273-301 , 2010.

[2] R.K. Barnhart, S.B. Hottman, D.M. Marshall, E. Shappee *Introduction to Unmanned Aircraft Systems*, 2012.

[3] T.H. Cox, C.J. Nagy *Civil UAV Capability Assessment*, December 2004.

[4] C. Nam, S. Danielson *Development of a Small UAV with real-time video surveillance*,American Society for Engineering Education, 2011.

[5] Department of Defense *Unmanned Systems Integrated Roadmap*, 2013.

[6] R. Beard, D. Kingston, M. Quigley, *Autonomous Vehicle Technologies for Small Fixed-Wing UAVs*, Journal of Aerospace Computing, Information and Communication, vol. 2, january 2005.

[7] J.W Langelaan *Long Distance/Duration Trajectory Optimization for small UAVs*,Guidance, Navigation and Control Conference, August, 2007.

[8] *Equations of Motion*, Flying Qualities Phase Textbook, vol. 2, chapter 4, 1988.

[9] F.R. Triputra, B.R. Trilaksono, R.A. Sasongko, *Longitudinal Dynamic System modeling of a Fixed-wing UAV towards autonomous flight control system development*, 2012 International Conference on system engineering and Technology, September, 2012.

[10] XFLR -5 *Analysis of foils and wings operating at low Reynolds numbers*, February, 2011.

[11] D. Jung, P. Tsiotras, *Modeling and Hardware-in-the-loop simulation for a small Unmanned Aerial Vehicle*, 2012.

[12] Aerovironment, *PUMA AE Overview Data Sheet* , October 2013.

[13] Aerovironment, *RAVEN AE Overview Data Sheet* , October 2013.

[14] MarcusUAV, *Zephyr2 UAV Overview Data Sheet* , 2013.

[15] A.M. Murch, B. Mettler, and G.L. Balas, *Frequency Domain system identification for a small, low-cost, fixed-wing UAV*, American Institude of Aeronautics and Astronautics.

[16] A. Noth, S. Bouabdallah, *Dynamic Modeling of Fixed-Wing UAVs*, October, 2008.

[17] J.B. Hostmark, *Modeling Simulation and Control of Fixed-wing UAV: CyberSwan*, June, 2007.

[18] E.J. Watkiss, *Flight Dynamics of an Unmanned Aerial Vehicle*, March, 1994.

[19] J. Manerowski, D. Rykaczewski, *Modelling of UAV flight dynamics using Perceptron artificial neural networks*, Journal of theoretical and applied mechanics, vol. 43, issue 2, pp. 297-307, 2005.

[20] X. Yang, L. Mejias and T. Molloy, *A Gust-attenuation Controller for Fixed-Wing UAV's during collision Avoidance Course*, 2012 International Conference on Unmanned Aircraft Systems, 2012.

[21] D.B. Kingston, R.W. Beard, *Real-Time Attitude and Postion Estimation for Small UAVs using Low-cost sensors*, 2012 International Conference on Unmanned Aircraft Systems, 2012.

[22] E.C. Papageorgiou, *Development of a dynamic Model for a UAV*, Naval Postgraduate, 1997.

[23] H.I. Leong, *Development of a 6DOF nonlinear simulation model enhanced with fine tuning procedures*, 2008.

APPENDIX

$$\begin{bmatrix} \dot{\alpha} \\ \dot{\beta} \\ \dot{p} \\ \dot{q} \\ \dot{r} \end{bmatrix} = \begin{bmatrix} q - (p\cos\alpha + r\sin\alpha)\tan\beta - \frac{1}{mV_T\cos\beta}(L + F_T\sin\alpha - mg(\sin\alpha\sin\theta + \cos\theta\cos\phi\cos\theta)) \\ p\sin\alpha - r\cos\alpha + \frac{1}{mV_T}(Y - F_T\cos\alpha\sin\beta + mg(\cos\alpha\sin\beta\sin\theta + \cos\beta\sin\phi\cos\theta - \sin\alpha\sin\beta\cos\phi\cos\theta) \\ c_1rq + c_2pq + c_3\bar{L} + c_4N \\ c_5qr - c_6p^2 + c_6r^2 + c_7M + c - 7F_TZ_Tp \\ c_8pq - c_2rq + c_4\bar{L} + c_9N \end{bmatrix}$$